Tactile Stimulation by Repetitive Lateral Movement of Midair Ultrasound Focus

Ryoko Takahashi, Keisuke Hasegawa, *Member, IEEE*, and Hiroyuki Shinoda, *Member, IEEE*

***Abstract*—We report a new vibrotactile modulation method of midair ultrasound focus, namely, lateral modulation (LM), in which the focus quickly moves along a small cyclic trajectory and provides stronger and clearer vibrotactile stimuli than those by the conventional amplitude modulation (AM) method. Midair ultrasound haptics has an essential technical advantage of offering remote, non-contact, and pinpoint tactile stimuli on device-free bare skin. On the other hand, lack of clarity in the presented vibrotactile sensation has often been pointed out, and until now, an AM focus has been valid only on glabrous skin. Our main scientific contribution of the article is to verify the LM method, with the following experimental findings newly obtained. We confirmed that with the same maximum output amplitude of the ultrasound phased arrays, LM stimuli with circular focal trajectories were sensed stronger than AM stimuli by glabrous skin and hairy skin in a modulation frequency of 10-200 Hz. We also found that the detection threshold in glabrous skin mainly depended on the focal speed, whereas the tendency in hairy skin was different from that. With these results, we discuss a basis of perceptional mechanism that responds to LM stimuli, along with practical aspects of potential applications.**

***Index Terms*—Midair haptics, haptic display, haptic perception, lateral modulation.**

I. Introduction

A. Ultrasound Midair Haptics

ACOUSTIC radiation pressure by a midair ultrasound focus can produce non-contact tactile stimuli on bare skin. Since this principle was first proposed and demonstrated [1], many devices and systems have been proposed based on the same. Phased array systems of ultrasound transducers have been developed by multiple groups [2], [3] since the advent of the first prototype of airborne ultrasound tactile display (AUTD) [1], [4]. Applications of this technology are diversified, and midair visuo-tactile interaction systems are developed wherein aerial tactile feedback is superimposed on floating images. An aerial touch panel with haptic feedback [5] and a visual and tactile clone system [6] would be representative examples of such systems. Thus, midair ultrasound haptics is actively studied owing to its essential advantage that it can instantaneously present a localized tactile sensation at an arbitrary position.

Manuscript received March 31, 2019; revised August 17, 2019; accepted September 16, 2019. Date of publication October 16, 2019; date of current version June 8, 2020. This work was supported in part by JSPS KAKENHI under Grant 16H06303 and in part by JST CREST under Grant JPMJCR18A2. This article was recommended for publication by Associate Editor F. Giraud upon evaluation of the reviewers' comments. *(Corresponding author: Keisuke Hasegawa.)*

R. Takahashi is with Dai Nippon Printing Company, Ltd, Tokyo 162-8001, Japan. (e-mail: takahashi@hapis.k.u-tokyo.ac.jp).

K. Hasegawa is with the Graduate School of Information Science and Technology, University of Tokyo13143, Tokyo 113-8656, Japan. (e-mail: keisuke_hasegawa@ipc.i.u-tokyo.ac.jp).

H. Shinoda is with the Graduate School of Information Science and Technology, University of Tokyo13143, Tokyo 113-8656, Japan and also with Graduate School of Frontier Sciences, University of Tokyo, Kashiwa 277-8561, Japan. (e-mail: hiroyuki_shinoda@k.u-tokyo.ac.jp).

Digital Object Identifier 10.1109/TOH.2019.2946136

B. Our Motivation

The possible greatest radiation pressure by the device can be attained by generating an ultrasound focus as implemented in most ultrasound midair haptics. The next technique to intensify the stimulation is to provide time-variant stimulation on skin. The validity of this approach relies on mechanism of human touch perception: several different types of mechanoreceptors selectively respond to stimuli according to their temporal characteristics. For this reason, the amplitude modulation (AM) of the output waveform has been prevalently used as the conventional method. In practice, waveforms containing 100 Hz or higher frequency components, to which the mechanoreceptors in glabrous skin sensitively respond, are used for amplitude modulation [7]. It is also known that the appropriately designed amplitude waveforms could offer particular vibrotactile textures [8]. Compared with non-modulated foci, AM foci offer subjectively enhanced vibrotactile stimuli. However, until now successful vibrotactile presentation has been limited to glabrous skin. In case of hairy skin, it has been difficult to present perceivable tactile sensation without strong attention of users or their voluntary (or exploratory) body movements. Increasing the radiation pressure by employing a larger number of transducers has been an evident solution for improving the focal intensity [7], [9]. Nevertheless, it is not always desirable to emit ultrasound of strong intensity from the viewpoint of power consumption and device cost.

We previously found a new modulation method that presents stronger and clearer vibrotactile stimuli on the skin surface than AM, while maintaining the number of transducers and their maximum output pressure [10], [11]. We called this method as lateral modulation (LM). In the case of the AM method, the intensity of a spatially fixed ultrasound focus temporally varies. In case of LM focus, ultrasound intensity is stationary while the focal position is time-variant. It produces vibrotactile stimuli by quick and repetitive focal movement along a short trajectory that is limited within a spatial dimension of several millimeters on skin and is

mostly perceived as directionless point vibrotactile stimulation. With the high-speed small focal movement, the user does not perceive a trail of focal movement but senses it as vibrotactile stimulus. The effect of lowering the vibration detection threshold with the LM method was observed among a wide range of modulation frequency between 10-200 Hz. The goal of this study is to verify the effectiveness of this method on both glabrous skin and hairy skin, with an enriched set of newly performed subject studies that included varied experimental parameters. In addition, the detailed conditions and mechanism of the LM method are discussed based on the obtained experimental results.

Unlike most of the current 'active' midair haptic applications which target the palm or fingertips, our new method will present perceivable vibrotactile stimuli to a wider range of body regions with hairy skin. This technical improvement will offer various practical 'passive' contents such as presentation of a tactile trigger calling user attention and tactile feedback to users during their voluntary body movements, without wearable devices [12], [13].

Note that, with AUTDs it is possible to generate multiple simultaneous foci or even specifically-shaped radiation pressure distribution, with properly calculated phase delays and amplitude differences among transducers [14], [15]. Nevertheless, we limit the scope of our study to the case of a single focus.

C. Physiological Views on Human Response to Moving Tactile Stimuli

A primary characteristic of the ultrasound midair haptics is that it generates radiation pressure perpendicular to the skin surface with no shear force. In contrast, tactile stimuli presented on direct contacts by the real object are not the case. For this reason, the report [16] that the stimulus perception intensity increases with the shear force is not applicable to our case.

It has been widely known that the frequency factor has a large influence on perceptual intensity in vibrotactile stimulus [17]. This tendency is also confirmed in midair ultrasound haptics [7]. As for the LM method, an ultrasound focus on its repetitive moving path causes mechanical vibration on individual mechanoreceptors, of which acoustic power on the entire skin is actually doubled, when compared with AM. However, our experiments showed that decrease in threshold cannot be explained merely by the increase in acoustic power, indicating that the movement of the stimulation point on skin inherently increases the subjective intensity of vibrotactile sensation [10].

We conducted several additional experiments apart from the practical aspect of LM, to clarify the perception of LM vibrotactile stimuli. We listed several specific factors that might affect tactile perception, and experimentally confirmed which ones are actually influential. Consequently, we found that the sensitivity of glabrous skin mainly depended on the speed of the focal point (hereinafter we just refer to it as the 'focus'). The detection threshold declined with the increase in focal speed while it was less than 2 m/s. This tendency was not observed in case of hairy skin. Integrating all those findings, we refer to a possibility that the LM focus might selectively stimulate a specific type of mechanoreceptors in the section of discussions.

II. Principle

A. Ultrasound Focusing With AUTD

An AUTD comprises ultrasound transducers arranged in a lattice pattern. The phase and amplitude of the output waveform of each transducer can be individually controlled. An AUTD concentrates acoustic power in a circular region that is referred to as a focus, with diameter comparable to the wavelength, depending on the focal depth and the emission aperture width [7]. The focusing is achieved when each transducer emits ultrasound with determined individual phase delay, thereby all outputs are in phase at the focal position. When a solid object blocks intense acoustic propagation inside a focus, positive pressure is generated on the object surface. This pressure is called acoustic radiation pressure [18], which offers non-contact tactile sensation on skin.

B. Conventional Vibrotactile Presentation Method: Amplitude Modulation (AM)

For generating infallibly detectable vibrotactile sensation, it is necessary to use a time-variant stimulus to the mechanoreceptors as stated above. Vibrotactile stimulation presentation by temporal AM of the ultrasound pressure has been widely used in ultrasound midair haptics [1]. The AM envelope of the carrier sinusoidal ultrasound waveform corresponds to vibrotactile stimulation waveform [4], [7]. The carrier frequency is 40 kHz for most cases (including our study), which is much higher than the upper limit of perceivable vibrotactile frequency for human. The driving signals to the transducers on AUTDs are provided from the digital outputs of field programmable gate arrays (FPGA) by using amplifiers with a fixed amplification coefficient. Output ultrasound amplitudes of transducers are tuned by changing the duty cycle of rectangle pulses from the FPGAs. This principle is partially similar to the pulse-width-modulation (PWM) technique [7]. The modulation waveform need not be sinusoidal, and it is known that an appropriately tuned waveform offers particular vibrotactile textures. Although this feature is useful in practical situations, we used sinusoidal modulations in the experiments based on numerous precedent studies [5], [7], [8]. In presenting vibrotactile stimuli with sinusoidal AM on the palm (glabrous skin), it is known that the vibration detection threshold is the lowest at around 200 Hz [7]. This is presumably due to the response of Pacinian corpuscles, which is observed most prominent around the vibration frequency of 200 Hz. However, it has been found difficult to perceive midair ultrasound vibrotactile stimuli on hairy skin with AM, especially when the modulation frequency exceeds 200 Hz.

C. Proposed Method: Lateral Modulation (LM)

The proposed LM method presents vibrotactile stimuli to skin by a focus that repetitively travels along a horizontal trajectory while keeping the intensity of radiation pressure constant. Fig. 1 shows comparative schematics depicting the concepts of the AM and LM methods. We define two specific LM methods based on the focal trajectories: (1) a periodical

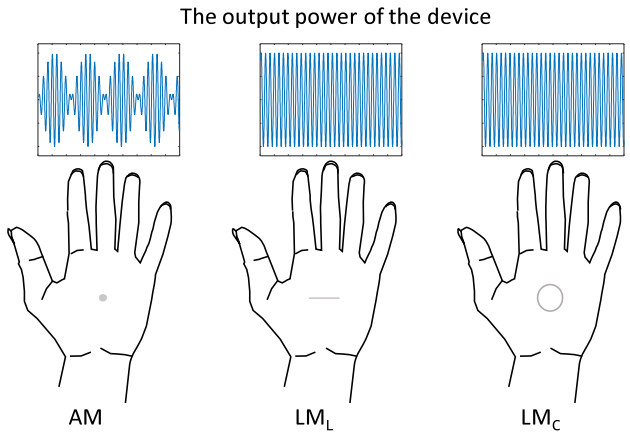

Fig. 1. Concepts of AM and LM methods. The waveforms indicate output waveform of instantaneous acoustic pressure from transducers and gray lines indicate focal trajectories for each case.

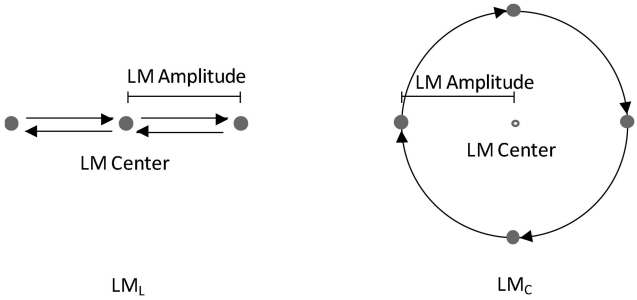

Fig. 2. Definition of LM terms.

linear movement that is referred to as LM$_L$, and (2) a periodical circular motion that is referred to as LM$_C$. For later discussions, several terms and parameters in LM are defined as follows (Fig. 2).

The LM center represents a center of the line segment in LM$_L$, while it is the center of the circle in LM$_C$. The LM amplitude in LM$_L$ is a half of the length of the line segment, while it is the radius of the circle in LM$_C$. In addition, we define LM frequency as the frequency of the cyclic movement of the focus. In the following part of the paper, we denote an LM stimulus with LM frequency of A Hz and LM amplitude of B mm as "(A Hz, B mm) LM."

Here we compare AM and LM based on a physical aspect. We demonstrate that LM will apply twice as much acoustic power to the entire skin in time average as AM, when the maximum presented pressure is identical. The instantaneous acoustic pressure at the focal point $p_{AM}(t)$ and $p_{LM}(t)$ are given as:

$$p_{AM}(t) = p_0 \sin(\omega_c t) \sin(\omega_m t)$$

$$p_{LM}(t) = p_0 \sin(\omega_c t),$$

where ω_c is the carrier angular frequency of the ultrasound wave, $\omega_m (< \omega_c)$ is the modulation angular frequency, t is time, and p_0 is the maximum amplitude. Their time-averaged acoustic powers P_{AM} and P_{LM} received from the device are given as:

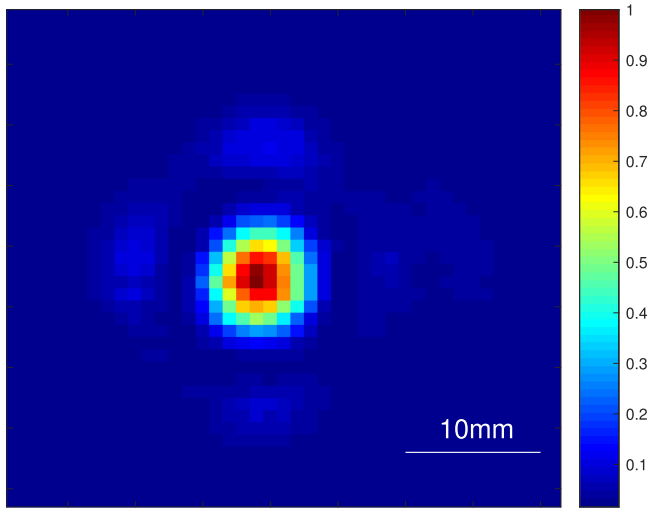

Fig. 3. Normalized squared acoustic pressure amplitude measured around the focus.

$$P_{AM} = \frac{a}{T}\int_0^T (p_{AM}(t))^2 dt$$

$$P_{LM} = \frac{a}{T}\int_0^T (p_{LM}(t))^2 dt.$$

Therefore, $P_{LM} = 2P_{AM}$. Here, a is a constant common to both equations and $T = \frac{2\pi}{\omega_m}$. Rigorously, it should be assumed that $\omega_c T = 2n\pi$ holds here for n being an integer.

Based on the above discussions, the LM frequency, the LM amplitude, and the orbit of the movement can be considered as possible independent factors affecting subjective LM stimulus intensity. In addition, we define the focal movement speed as follows. Let f be the LM frequency and l be the LM amplitude. In the experiment, we set the horizontal focal displacement of LM$_L$ and LM$_C$ respectively in a parametric fashion as $(x_L, y_L) = (l\cos\omega_m t, 0), (x_C, y_C) = (l\cos\omega_m t, l\sin\omega_m t)$, where t denotes time and $\omega_m = 2\pi f$. This means that the focal moving speed varies in relation to time with LM$_L$ in a sinusoidal fashion, whereas it is stationary with LM$_C$. The average speed of the focus is calculated as $v_L = 4lf$ for LM$_L$ and $v_C = 2\pi lf$ for LM$_C$, by which we define the focal movement speed. Note that they are calculated as averaged absolute value of speed and are not independent experimental parameters since they are products of LM amplitude and frequency.

Fig. 3 shows measurement of an acoustic field around the ultrasonic focus generated by the AUTDs. The measurement was done in a plane that was parallel to the emission plane of the AUTDs and was apart from it by 200 mm. The acoustic pressure was captured by a standard microphone system (Microphone: Type 4138-A-015, Preamplifier: Type 2670, Condition Amplifier: Type 2690-A, all product of Brüel & Kjær) mounted on an orthogonal scanning robot (ICSB3 Series, product of IAI Corporation). In general, the radiation pressure is in proportion to the acoustic power i.e. squared RMS value of sound pressure [18]. The size of the focal spot is observed to be comparable to the wavelength (8.5 mm).

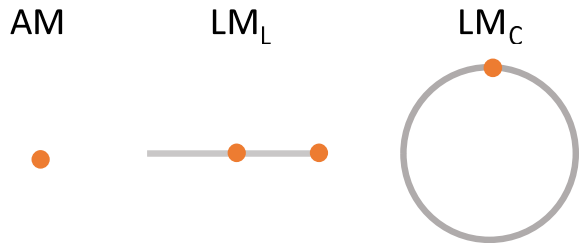

Fig. 4. The measurement points (orange dots) and focal orbits (gray lines) in Experiment 1.

Note that the vibration waveform on the skin might contain certain harmonics of LM frequency, as the focus has a specific spatial radiation pressure distribution (as depicted in Fig. 3). In addition, there is some portion on the LM focal trajectory where the second harmonics is prominently observed. This occurs because the focus moves across the center of the path twice in one cyclic motion as evident in the following experimental results.

III. Experimental Methods

We constructed an experiment workspace with 4 AUTD units mounted on the ceiling of an aluminum frame (Fig. 5). The size of the ultrasound emission plane was $384.0 \times 302.8\,\mathrm{mm}^2$. The total number ofxd transducers included in the workspace was 996. All experiments were performed at this defined workspace. The distance from the emission plane of the AUTD to the target was set to approximately 200 mm. For each participant, we configured the focal depth through interactive procedures with the participant in order to provide the strongest vibrotactile sensation. These procedures were necessary to compensate the effect of difference in the diameter of the individiual participants' forearms and the thickness of their palms.

Initially, we measured radiation pressure waveforms on several points at different focal trajectories. Then we conducted experiments with human participants for determining the detection threshold of the vibrotactile stimuli provided by an AM, LM$_L$, and LM$_C$ focus, while varying the focal parameters and output intensity. In presenting LM stimuli, the focal position was updated at 1 kHz. The subjects wore headphones that played white noise to cancel out auditory clues from modulated high-power ultrasound emission. To insulate body of the participants from the vibration of the device and fix the stimulation position, we placed one cushion located at the center of the workspace and asked the participants to lay one of their palms. When stimulating a forearm, we placed two cushions under it. We had 6 male and 4 female subjects, with age of 22-25 years. All of them were Japanese and their forearms are covered with thin hair on the whole. The experiments were approved by the Ethical Committee at the University of Tokyo, Japan. In all experiments, forearms and palms were stimulated as a representative hairy and glabrous body part. Therefore the obtained results of the following experiments may not be applied perfectly to other body parts.

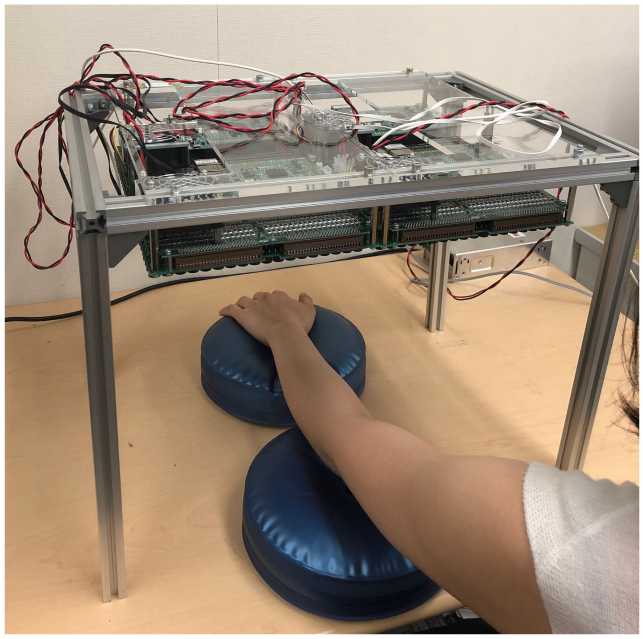

Fig. 5. A view of the experiments.

A. *Experiment 1: Measurement of Acoustic Radiation Pressure on a Fixed Point*

The first experiment was carried out as the waveform measurement of acoustic pressure generated by the LM method, with an electret condenser microphone (ECM) (KECG2738PBJ-A, a product of Kingstate, Taiwan) on a fixed position. The measured acoustic waveform was recorded by an oscilloscope (PicoScope 4262, a product of Pico Technology, UK). Radiation pressure is modulated with a time constant significantly longer than the period of the ultrasound oscillation [18]. Therefore, all the waveforms shown in this section were processed by the software (low-pass filter implemented in PicoScope) with its cut-off frequency set to 2,000 Hz to leave the radiation pressure and remove the carrier signal.

Fig. 4 shows the four measurement points of ultrasound, located on the three focal orbits: AM, LM$_L$ and LM$_C$. They are fixed on; 1) the stationary sinusoidal AM focus, 2) the center of the LM$_L$ orbit, 3) one of the end points in the LM$_L$ orbit, and, 4) one point on the LM$_C$ orbit, respectively. The modulation frequency was set to 25 Hz in all conditions. The LM amplitude was set to 7 mm.

Note that in this experiment, the modulation frequency did not need to match the ones chosen in the following experiments. The aim of this experiment is just to evaluate the magnitudes of harmonics that emerge in relation to modulation modes at a located spot.

B. *Experiment 2: Subjective Evaluation of Two Vibrotactile Stimuli*

In this experiment, the participants evaluated the difference between AM and LM$_C$ stimuli by subjective impressions. The reason we initiated with LM$_C$ is that it has smaller harmonic effect compared with LM$_L$. We presented AM and 7 mm LM$_C$ stimuli at the maximum intensity in the middle of the hairy part

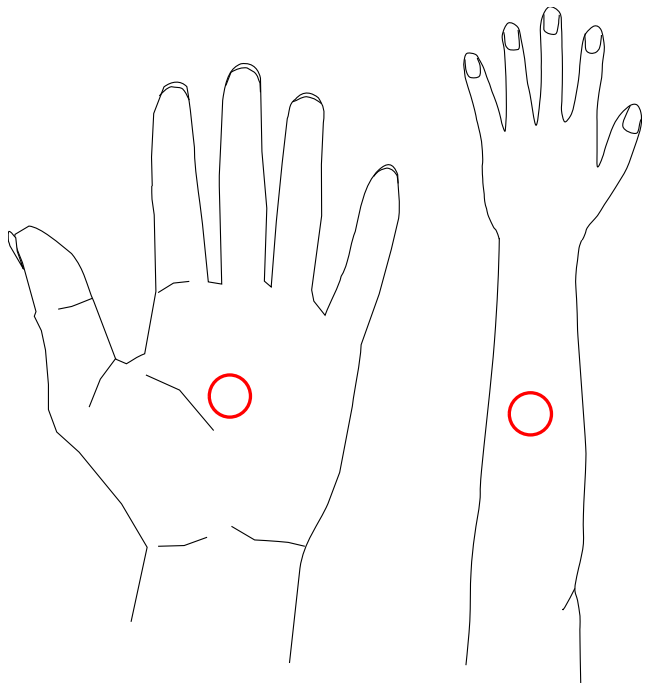

Fig. 6. The focus point in Experiments 3 and 4.

of their forearm, sequentially in a random order (Fig. 5). For both stimuli, the modulation frequency was 50 Hz, which had been confirmed to be easily detectable beforehand. After two stimuli were presented, the 10 participants were asked which stimulus was stronger. No equivocal answer was permitted.

C. Experiment 3: Vibration Detection Threshold of AM and LM_C Stimuli

We experimentally obtained the vibrotactile detection threshold of AM and LM_C stimuli on glabrous skin and hairy skin with respect to several modulation frequencies and LM amplitudes.

In the experiment, we stimulate the palm of the left hand (glabrous skin) and the center of the left forearm (hairy skin). Fig. 6 depicts the locations of the focal points on them. The experimental procedure was as follows.

1) Constant static pressure was initially presented on the skin
2) A vibrotactile stimulus was initiated with cue sound (a bell ringing) played by the headphone
3) Participants responded whether they felt vibration

In the experiment, negative radiation pressure was impossible to generate, it means that, the radiation pressure was always positive regardless of modulation modes. Here, negative radiation pressure refers to suction pressure on skin. In order to subtract the effect of this time-average offset pressure from the vibrotactile perception of participants, we initially presented static pressure that was set equal to the time-average in comparison with the subsequent vibrotactile stimulus. We produced the ultrasound focus so that the presented radiation pressure yielded no perceivable spatiotemporal discontinuity at the transition from the static pressure to the vibrotactile stimuli.

We defined the stimulus intensity by the maximum instantaneous output radiation pressure and altered it among 51 levels in the experiment, where the highest level corresponded to the maximum output and the lowest corresponded to null output. As shown in Fig. 1, the intensity of radiation pressure is time-invariant except in the case of AM. The acoustic power applied to the entire skin surface differs between the case of AM and LM_C for same stimulus intensity: as demonstrated in Section II-C, it is doubled in the case of LM_C. We obtained the detection threshold for each condition by using the method of limits. For each condition, the trial was done once in order to limit the experimental duration within two hours for mitigating the burden of participants, who were instructed to keep their posture still throughout the experiments. We set the modulation frequency to 10 Hz, 50 Hz, 100 Hz, and 200 Hz for the AM and LM_C stimuli. For glabrous skin, the LM amplitude was set to 1 mm, 3 mm, 5 mm, and 7 mm. For hairy skin, the condition of LM amplitude 1 mm was excluded, as most of the participants could not perceive the stimuli even at the maximum device output.

Preliminary experiments demonstrated that for the LM frequency of 50 Hz or higher, horizontal movement of LM_C foci with 7 mm amplitude were perceived as directionless vibration. For a 10 Hz-modulated LM_C focus with 7 mm amplitude, some participants perceived its spatial movement.

D. Experiment 4: Vibration Detection Threshold of LM_C and LM_L Stimuli

As will be described later, the results of Experiment 3 indicated that the perceptual intensity depended on the experimental parameters of LM_C. In order to investigate whether this tendency depended on focal trajectories, further experiments with different movement patterns (LM_L) were conducted.

We experimentally obtained the vibration detection threshold of LM_L stimuli on the palm. The same participants who engaged in Experiment 3 performed in the similar manner to that experiment. The LM frequency was set to 10 Hz, 50 Hz, 100 Hz, and 200 Hz, and the LM amplitude was set to 1 mm, 3 mm, 5 mm, and 7 mm.

IV. Experimental Results

A. Experiment 1

Fig. 7 shows the waveforms measured by the ECM. Waveforms with the common fundamental frequency of 25 Hz (corresponding to a period of 40 ms) were observed in all cases. At the center point of LM_L, a second harmonic is observed prominent, which is consistent with the expectation aforementioned in Section II-C. Thus, it was confirmed the doubled frequency effect is dominant only in the case of LM_L.

B. Experiment 2

In this experiment, all of the participants answered that LM_C was stronger. The aim of this preliminary experiment is just to confirm that LM_C stimuli is infallibly felt as stronger than AM, when both of them are at their maximum intensity.

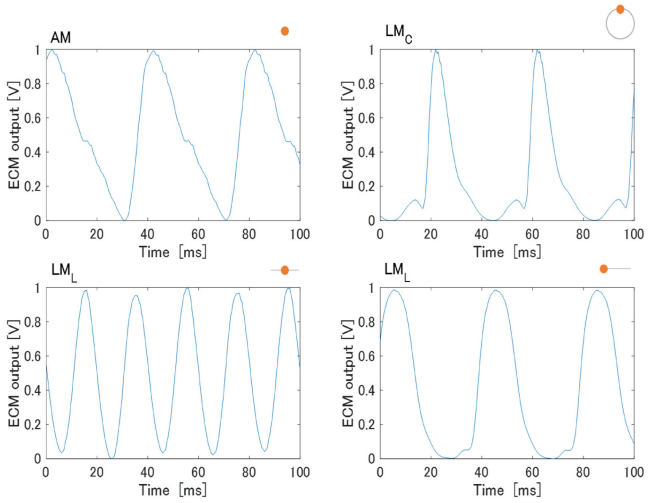

Fig. 7. The captured ECM output waveforms for each modulation method and measurement location. The waveforms were normalized.

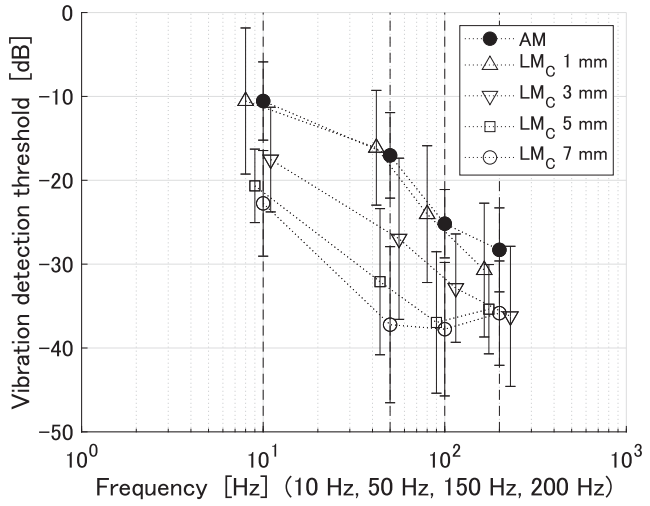

Fig. 8. Comparison of the average thresholds for AM and $\mathrm{LM_C}$ on glabrous skin. 0 dB corresponds to the upper limit of the output of the device. Error bars indicate the standard deviations.

C. Experiment 3

1) Results on Glabrous Skin: Fig. 8 shows the results on the palm. Here, 0 dB corresponds to the maximum device output. At first, we tested the obtained $\mathrm{LM_C}$ data sets by the Shapiro-Wilk test and found that all of them except the one with a condition of (100 Hz, 5 mm) followed the normal distribution ($p \geq 0.05$).

The maximum difference in detection threshold between AM and $\mathrm{LM_C}$ of the same frequency was 20.2 dB with (50 Hz, 7 mm) $\mathrm{LM_C}$ stimuli. The thresholds of 3 mm, 5 mm and 7 mm $\mathrm{LM_C}$ stimuli for all frequencies were significantly different from that of AM in the paired t-test ($p = 2.6 \times 10^{-3}$ at the greatest for (200 Hz, 3 mm), and $p = 1.0 \times 10^{-6}$ at the least for (50 Hz, 7 mm)). We performed two-way repeated measures ANOVA with detection thresholds for $\mathrm{LM_C}$ stimuli alone, where LM amplitude and LM frequency are the factors. We found that both of the factors significantly affected the threshold ($p = 4.1 \times 10^{-12}$ for LM amplitude, and $p = 1.4 \times 10^{-18}$ for LM frequency): as the LM frequency or amplitude increased, the threshold was lowered. This can be explained with the frequency response characteristics of Pacinian corpuscles and is consistent with previous studies using AUTD [7]. There were no interaction demonstrated in ANOVA.

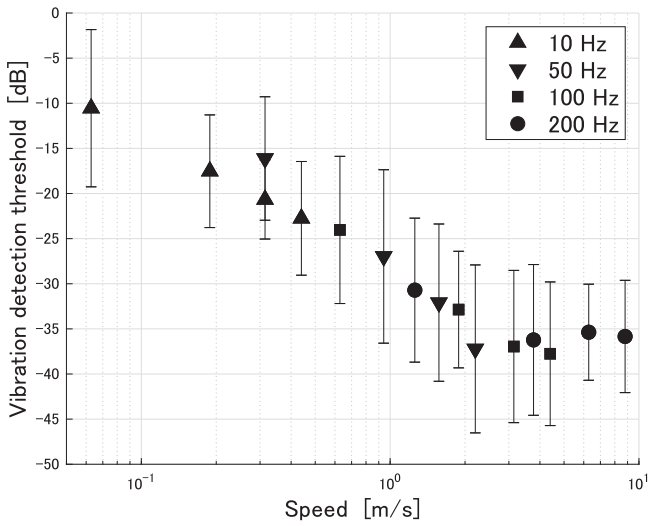

Fig. 9. The average thresholds of $\mathrm{LM_C}$ on glabrous skin, plotted against moving speed of focus. Error bars indicate the standard deviations.

In the experiments, LM amplitude and frequencies were independent experimental variables. As mentioned in Section II-C, the focal speed is defined as a product of an LM amplitude and an LM frequency. The speed values used in the experiments are: 0.06, 0.19, 0.31 (two combinations, 1 mm/50 Hz and 5 mm/10 Hz), 0.44, 0.62, 0.94, 1.26, 1.57, 1.88, 2.20, 3.14, 3.77, 4.40, 6.28 and 8.80 m/s. We also performed one-way ANOVA with the focal speed as the factor. The null hypothesis here is that the focal speed does not affect the mean value of the threshold when it is assumed to follow the normal distribution. As a result the null hypothesis is rejected ($p = 1.2 \times 10^{-20}$). Figs. 9 and 10 show the thresholds of $\mathrm{LM_C}$ alone, plotted against the focal movement speed and stimulation area, respectively. The stimulation area here is defined as the area included in a moving circular region with its origin tracing the focal trajectory, during one cycle of focal movement. The circular region corresponds to the focus and hence its diameter is equal to the wavelength (8.5 mm). The area is given as $S_{\mathrm{LM_C}} = \pi(l + r)^2$, where l and r denote the LM amplitude and the wavelength, respectively. As understood by its definition, stimulation area is essentially equivalent to the LM amplitude. It is observed that the thresholds were monotonically lowered with the increase in the speed until the speed reached around 2 m/s. (Fig. 9). An interesting tendency observed here is that when the values of focal speeds are close to one another, corresponding threshold values are also close to one another, regardless of the LM frequency (and amplitudes). From this result, it is conjectured that the focal speed might be a more definitive factor for threshold than LM amplitude or frequency alone. In the contrast, it is observed that the size of the stimulus area is not as definitive as the focal speed due to remaining influence of the LM frequency (Fig. 10).

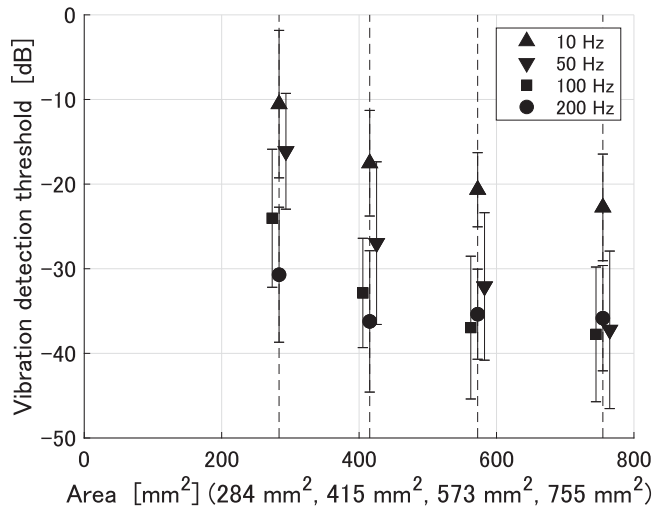

Fig. 10. The average thresholds of LM_C on glabrous skin plotted against stimulation areas. Error bars indicate the standard deviations.

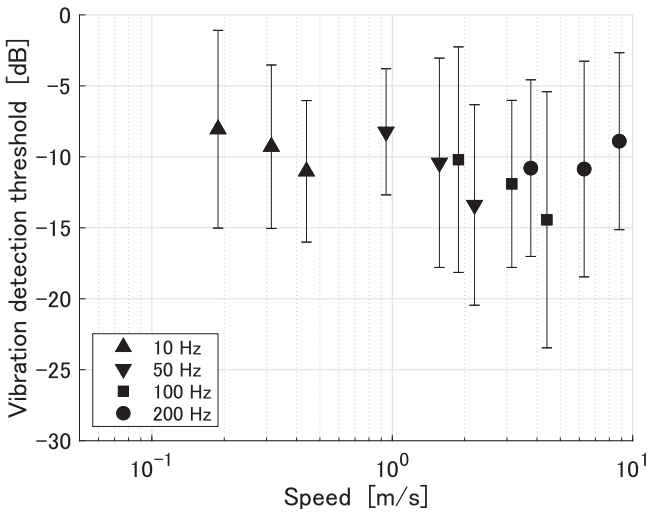

Fig. 12. The average thresholds of LM_C on hairy skin plotted against focal moving speeds. Error bars indicate the standard deviations.

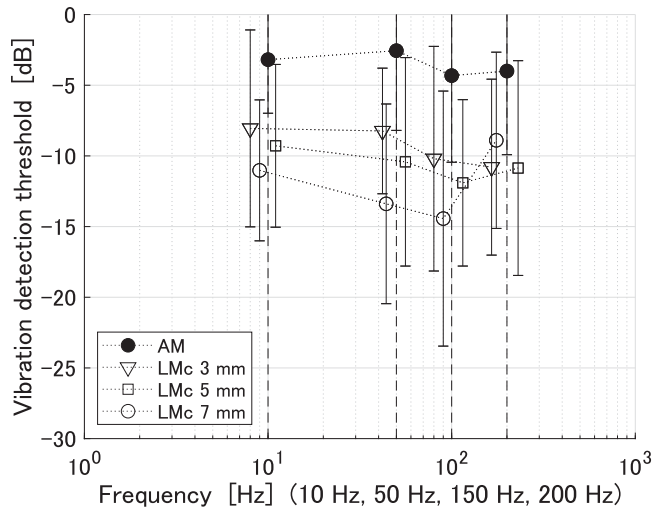

Fig. 11. Comparison of the average thresholds between AM and LM_C on hairy skin plotted against modulation frequencies. Error bars indicate the standard deviations.

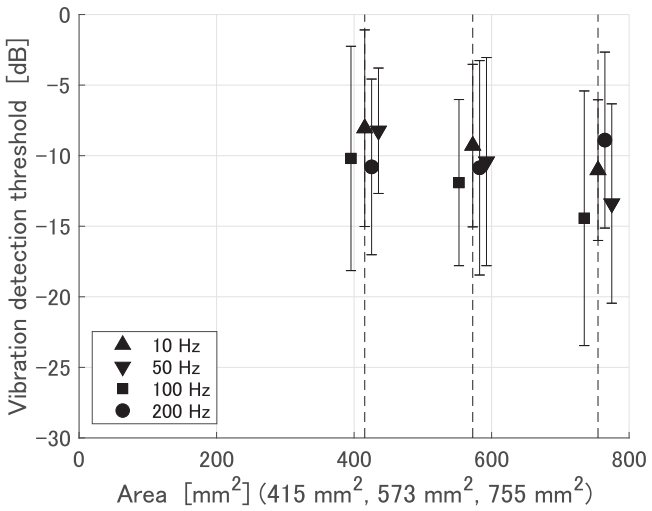

Fig. 13. The average thresholds of LM_C on hairy skin plotted against stimulation areas. Error bars indicate the standard deviations.

2) Results on Hairy Skin: Fig. 11 shows the result for the forearm. The cases in which vibration was not felt even at the maximum output were uniformly counted as thresholds of 0 dB (maximum output). AM stimuli at 100 Hz could not be felt by two participants and 10 Hz, 50 Hz, and 200 Hz AM stimuli could not be felt by three participants. The maximum difference in detection threshold between AM and LM_C of the same frequency was 10.8 dB with (50 Hz, 7 mm) LM_C stimuli. The threshold of all LM_C stimuli were significantly different from the AM of the same modulation frequency in the paired t-test ($p = 1.4 \times 10^{-2}$ at the greatest for (10 Hz, 3 mm), and $p = 9.8 \times 10^{-7}$ at the least for (10 Hz, 7 mm)).

We performed two-way repeated measures ANOVA in a similar fashion as with glabrous skin. As a result, neither LM frequency nor amplitude had significant influence on threshold. Next, we performed a one-way ANOVA with the focal speed as a factor. The null hypothesis was not rejected ($p \geq 0.05$) that the mean value of threshold is irrespective of the focal speed when the threshold is assumed to follow the normal distribution. Figs. 12 and 13 shows the results of LM_C alone, plotted against focal movement speed and stimulation area. In contrast to the result of glabrous skin, the obtained thresholds were irrespective of those factors.

D. Experiment 4

Fig. 14 shows the results of LM_L and LM_C stimuli, plotted against focal movement speed. The speed values are: 0.04, 0.12, 0.2 (two combinations, 1 mm/50 Hz and 5 mm/10 Hz), 0.28, 0.4, 0.6, 0.8, 1, 1.2, 1.4, 2, 2.4, 2.8, 4 and 5.6 m/s. Regardless of the focal movement pattern, the threshold tended to be on a single line decreasing monotonically for a speed less than 2 m/s, and the distribution of the LM_L and LM_C threshold against the focal speed roughly overlapped one another. At a faster speed, the increase in the focal movement speed was seen less influential in

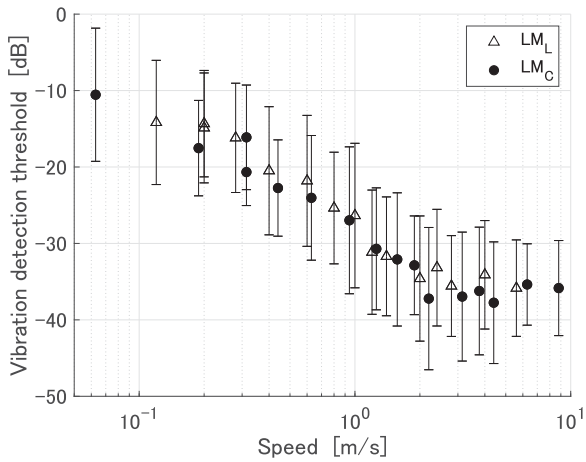

Fig. 14. The average thresholds of LM_L and LM_C on glabrous skin plotted against focal moving speeds. Error bars indicate the standard deviations.

the threshold. We tested the obtained LM_L data sets by the Shapiro-Wilk test and found that all of them normally distributed ($p \geq 0.05$). A one-way ANOVA demonstrated that LM_L focal speed significantly affected the threshold ($p = 4.4 \times 10^{-21}$). Due to the differences in experimental procedures between this and the LM_C detection task where AM stimuli were intermittently presented, direct comparison of LM_L and LM_C plots may be somewhat inappropriate. Nevertheless, it is notable that a similar focal-speed-dependency of detection threshold was observed regardless of focal trajectory shapes.

V. Discussion

For both glabrous skin and hairy skin, it was demonstrated that the lateral modulation is effective in significantly lowering the detection thresholds among a wide range of modulation frequencies, compared with the conventional AM method. This cannot be ascribed to the doubled acoustic power in LM that only corresponds to difference of 6 dB in AM stimulus intensity, which is smaller than the observed reduction in thresholds. In addition, effects of second harmonics occurring in LM_L were not dominant on the threshold in glabrous skin. Based on the evidences from the experiments, we conclude that the movement of the stimulation point on the skin inherently increases the sensitivity. Thus the LM method is more advantageous than the AM in terms of device power consumption. Our results indicate that geometries of focal path are less likely to affect the threshold, according to the similarity of threshold curve obtained with LM_L and LM_C cases.

There are two possible factors that explain this speed-dependence of the threshold. The first possibility is a physical effect on the skin [19]. In that study, it is demonstrated that the focal movement speed affected subjective intensity of stimuli, which was maximized when the focal speed matched the transmission velocity of the surface wave on the skin. In this situation, the consecutively produced wave fronts of moving foci are expected to interfere with one another, resulting in amplified vibrotactile stimuli. In that study, the tactile sensation was the strongest around the focal speed of approximately 8 m/s. The experiment is conducted with multiple focal velocities ranging from 2 m/s to 20 m/s, which conforms to our result. In case of the spatial vibrotactile stimuli, there is a possibility that the same result can be obtained in that range (2-20 m/s) of focal speed.

The second one is a physiological possibility where a perceptional mechanism that selectively responds to tactile stimuli, that move on the skin surface. Previous study of a moving brush on glabrous skin of fingers of the participants [20] demonstrated that the average firing rate of the Meissner corpuscles is correlated with the speed of the brush sweeping the finger. The experimental setup and obtained results of this study are similar to our research, but the brush used in that study yielded shear force while ultrasound foci do not. Therefore, it is clearly indicated that spatial movement of the stimuli even without shear force can promote the firing of the receptors.

From our experimental results, it is assumed that the LM stimuli may selectively stimulate Meissner corpuscles that are sensitive to the temporal derivative of the applied stress. This is explained by the fact that the sum of the pressures given within the area of focal movement is constant and that the receptive field sizes of Pacinian and Meissner corpuscles are different: deeply positioned receptors (Pacinian corpuscles) receive an aggregate of stimuli in a wide area. They are insensitive to minute spatial changes in presented stimuli. Furthermore, it was experimentally confirmed that the essential factor about perception of LM stimuli is the speed of moving stimuli, rather than the modulating frequency. The perception intensity monotonically increases with the increase in the focal speed. This tendency continues until the speed reaches 2 m/s, where the responses of the Meissner corpuscles may be saturated. It is conjectured that this tendency was not applied to hairy skin, where hair follicles play a role of mechanoreceptors. They differ from the Meissner and Pacinian corpuscles in the physical and physiological aspect [21].

Selective stimulation leads to reconstruction of a texture with reality [22], [23]. Combined with the AM method that is expected to mainly stimulate Pacinian corpuscles owing to its spatially stationary manner, there is a possibility that such a texture would be created in midair haptics.

Generation of high-intensity ultrasound field accompanies localized wind flows known as acoustic streaming, which is another representative nonlinear acoustic phenomenon besides radiation pressure. Hence the tactile stimulation in the experiment is a mixture of radiation-pressure-based vibration and wind flows. A possibility should be noted that vibrotactile component derived from turbulent acoustic streaming might be exist, which is irrelevant of designed AM or LM vibrotactile stimuli. Nevertheless, we consider the effect of the streaming as not very significant because of experimentally validated focal-speed-dependence of detection thresholds.

VI. Conclusion

We proposed the lateral modulation (LM) as a new method to present midair ultrasound vibrotactile stimuli. We verified the effectiveness of the LM method in terms of enhancing the

subjective strength of the presented vibrotactile stimuli both on glabrous skin and hairy skin, compared with the conventional AM methods. We demonstrated that this effect was valid for modulations of 10-200 Hz. In discussions, we referred to the possibility that each modulation mode (LM and AM) may selectively stimulate different types of mechanoreceptors, based on the obtained experimental results and fundamentals of haptic physiology.

This method can present a clearly perceivable vibrotactile stimulus to forearms, which is a representative body part covered by hairy skin. The result would be utilized to develop full-body haptics systems after further investigations of thresholds in other body regions. The results also suggest the facts about tactile stimuli without shear force that the speed of the moving stimulation has a large influence on the perception intensity. In addition, it is important to set the speed of moving stimuli above 2 m/s in order to ensure sufficient strength when designing the spatial vibrotactile stimulus to glabrous skin. Our future challenges include the designing of tactile textures based on the combination of LM and AM methods by investigating by what means each modulation affects our texture perception, in addition to the practical implementation of passive whole-body haptic system based on the LM method.

REFERENCES

[1] T. Iwamoto, M. Tatezono, and H. Shinoda, "Non-contact method for producing tactile sensation using airborne ultrasound," in *Haptics: Perception, Devices and Scenarios*, M. Ferre, Ed., Cham, Switzerland: Springer, 2008, pp. 504–513.

[2] G. Korres and M. Eid, "Haptogram: Ultrasonic point-cloud tactile stimulation," *IEEE Access*, vol. 4, pp. 7758–7769, 2016.

[3] T. Carter, S. A. Seah, B. Long, B. Drinkwater, and S. Subramanian, "Ultrahaptics: multi-point mid-air haptic feedback for touch surfaces," in *Proc. 26th Annu. ACM Symp. User Interface Softw. Technol.*, 2013, pp. 505–514.

[4] T. Hoshi, M. Takahashi, T. Iwamoto, and H. Shinoda, "Noncontact tactile display based on radiation pressure of airborne ultrasound," *IEEE Trans. Haptics*, vol. 3, no. 3, pp. 155–165, Jul.–Sep. 2010.

[5] Y. Monnai, K. Hasegawa, M. Fujiwara, K. Yoshino, S. Inoue, and H. Shinoda, "Haptomime: Mid-air haptic interaction with a floating virtual screen," in *Proc. 27th Annu. ACM Symp. User Interface Softw. Technol*, 2014, pp. 663–667.

[6] Y. Makino, Y. Furuyama, S. Inoue, and H. Shinoda, "Haptoclone (haptic-optical clone) for mutual tele-environment by real-time 3D image transfer with midair force feedback," in *Proc. CHI Conf. Human Factors Comput. Syst.*, 2016, pp. 1980–1990.

[7] K. Hasegawa and H. Shinoda, "Aerial vibrotactile display based on multiunit ultrasound phased array," *IEEE Trans. Haptics*, vol. 11, no. 3, pp. 367–377, Jul.–Sep. 2018.

[8] K. Hasegawa and H. Shinoda, "Aerial display of vibrotactile sensation with high spatial-temporal resolution using large-aperture airborne ultrasound phased array," in *Proc. World Haptics Conf.*, Apr. 2013, pp. 31–36.

[9] S. Suzuki, R. Takahashi, M. Nakajima, K. Hasegawa, Y. Makino, and H. Shinoda, "Midair haptic display to human upper body," in *Proc. SICE Annu. Conf.*, 2018, pp. 848–853.

[10] R. Takahashi, K. Hasegawa, and H. Shinoda, "Lateral modulation of midair ultrasound focus for intensified vibrotactile stimuli," in *Haptics: Perception, Devices and Scenarios*, M. Ferre, Ed., Cham, Switzerland: Springer, 2018, pp. 276–288.

[11] R. Takahashi, S. Mizutani, K. Hasegawa, M. Fujiwara, and H. Shinoda, "Circular lateral modulation in airborne ultrasound tactile display," in *Haptic Interaction*, H. Kajimoto, D. Lee, S. Y. Kim, M. Konyo, and K. U. Kyung. (Eds.), AsiaHaptics 2018, Lecture Notes in Electrical Engineering, vol. 535, 2018. [Online]. Available: https://doi.org/10.1007/978-981-13-3194-7_20

[12] Teslasuit, 2019. [Online]. Available: http://teslasuit.io/

[13] NullSpace VR, 2019. [Online]. Available: http://nullspacevr.com/

[14] B. Long, S. A. Seah, T. Carter, and S. Subramanian, "Rendering volumetric haptic shapes in mid-air using ultrasound," *ACM Trans. Graph.*, vol. 33, no. 6, pp. 181:1–181:10, 2014.

[15] S. Inoue, Y. Makino, and H. Shinoda, "Active touch perception produced by airborne ultrasonic haptic hologram," in *Proc. IEEE World Haptics Conf.*, 2015, pp. 362–367.

[16] V. Hayward and M. Cruz-Hernandez, "Tactile display device using distributed lateral skin stretch," in *Proc. Haptic Interfaces Virtual Environ. Teleoperator Syst. Symp.*, 2000, vol. 69, no. 2, pp. 1309–1314.

[17] A. Gescheider, S. J. Bolanowski, and K. R. Hardick, "The frequency selectivity of information-processing channels in the tactile sensory system," *Somatosensory Motor Res.*, vol. 18, no. 3, pp. 191–201, 2001.

[18] M. F. Hamilton and D. T. Blackstock, *Nonlinear Acoustics*. San Diego, CA, USA: Academic, 1998, vol. 237.

[19] W. Frier *et al.*, "Using spatiotemporal modulation todraw tactile patterns in mid-air," in *Haptics: Perception, Devices and Scenarios*, M. Ferre, Ed., Cham, Switzerland: Springer, 2018, pp. 270–281.

[20] G. K. Essick and B. B. Edin, "Receptor encoding of moving tactile stimuli in humans. II. The mean response of individual low-threshold mechanoreceptors to motion across the receptive field," *J. Neuroscience*, vol. 15, no. 1, pp. 848–864, 1995.

[21] D. M. Bautista and E. A. Lumpkin, "Perspectives on: Information and coding in mammalian sensory physiology," *J. General Physiol.*, vol. 138, no. 6, pp. 653–653, 2011.

[22] N. Asamura, N. Yokoyama, and H. Shinoda, "Selectively stimulating skin receptors for tactile display," *IEEE Comput. Graph. Appl.*, vol. 18, no. 6, pp. 32–37, Nov./Dec. 1998.

[23] M. Konyo, S. Tadokoro, A. Yoshida, and N. Saiwaki, "A tactile synthesis method using multiple frequency vibrations for representing virtual touch," in *Proc. IEEE/RSJ Int. Conf. Intell. Robots Syst.*, 2005, pp. 3965–3971.

Ryoko Takahashi received the B.E. degree in engineering and the M.S. degree in information science and technilogy from the University of Tokyo, Tokyo, Japan, in 2017 and 2019, respectively. She is currently with Dai Nippon Printing Company, Ltd, Tokyo, Japan. Her research interests include haptics, focusing on ultrasound haptics, and tactile perception.

Keisuke Hasegawa (M'13) received the B.E. degree in information physics and the M.E. and Ph.D. degrees in information science and technology from the University of Tokyo, Tokyo, Japan, in 2009, 2011, and 2014, respectively. He is currently a Research Associate with the Graduate School of Information Science and Technology, University of Tokyo. He was a Postdoc Researcher in 2014 and a Project Research Associate from 2015 to 2018 with the University of Tokyo. His current research interests include haptic technologies, applied physics, and human-oriented informatics.

Hiroyuki Shinoda (M'09) received the B.S. degree in applied physics, the M.S degree in information physics, and the Ph.D. degree in engineering from the University of Tokyo, Tokyo, Japan, in 1988, 1990, and 1995, respectively. He is a currently Professor with the Graduate School of Frontier Sciences, University of Tokyo. He was an Associate Professor with the Department of Electrical and Electronic Engineering, Tokyo University of Agriculture and Technology. After a period with UC Berkeley, as a Visiting Scholar in 1999, he was an Associate Professor with the University of Tokyo from 2000 to 2012. His research interests include information physics, haptics, mid-air haptics, two-dimensional communication, and application systems related to them. He is a member of IEEJ, RSJ, JSME, and ACM.